Environmental Earth Sciences (2022) 81: 422
https://doi.org/10.1007/s12665-022-10547-x

THEMATIC ISSUE

Late Quaternary palaeoenvironmental controls on concentric talus evolution in the Central Ebro Basin (NE Spain)

José Luis Peña-Monné[1] · María Marta Sampietro-Vattuone[2] · Jesús V. Picazo-Millán[3]

Received: 10 February 2022 / Accepted: 6 August 2022 / Published online: 23 August 2022

Abstract

The polyphasic evolution of the testimonial buttes in the central area of the Ebro basin (Los Monegros) is analysed. This is a semiarid area that favours high erosion rates. An evolutionary model of the Jubierre hills is presented that shows the environmental cycles represented by aggradational and degradative processes on the slopes that resulted in the present arrangement of talus flatiron rings. In the four studied cases, talus relicts are composed of detritic material from a disappeared caprock pediment. Four slope stages (S4 to S1) that formed under stable climate conditions are identified. Older stages (S4 and S3) are estimated by comparison with other talus flatirons in the region. The S2 stage contains Bronze Age archaeological remains and the radiocarbon age obtained was 1608–1446 years cal BC (2σ), while S1 is younger. A palaeoenvironmental interpretation was made for these aggradational stages (S4 to S1). The active erosion of these hills led to a relief inversion, and talus flatirons remain as the only features revealing the presence of the relict hills and past human occupations.

Keywords Holocene · Talus flatiron · Erosion · Geoarchaeology · Semiarid environment

Introduction

The central sector of the Ebro basin (NE Spain) is composed of Miocene sediments that underwent a complex and varied geomorphological evolution after opening to the Mediterranean Sea in the Upper Miocene (Gutiérrez and Peña Monné 1993). Its climate favours semiarid processes and landforms. One of the most outstanding features is the cyclical character of many of the landscape morphologies following environmental changes and human activities (Peña Monné et al. 2000, 2004; Peña Monné 2018). The best expression of these cycles is the evolution of slopes during the Holocene (Sancho et al. 1988; Gutiérrez et al. 2010, 2015).

The centre of the Ebro depression followed a classic evolution of horizontal or sub-horizontal structures (tablelands) (Duszinsky et al. 2019). The incision of the Ebro River and its tributaries caused the subdivision of the tablelands into plateaus and mesas. These morphologies are characterised by an upper resistant caprock of sandstones and limestones, and a weaker talus lower rock that is segmented by minor structural steps (Duszinsky et al. 2019). These landforms progressively evolve to smaller landforms (from plateau to mesa, butte, and finally pinnacle) (Migoń et al. 2018, 2019, 2020) through slope retreat. In the final stages, these landforms lose their hard caprocks to form hills degraded by erosion and badlands (Boroda et al. 2011, 2014; Migoń et al. 2018).

In all these evolutionary stages, but essentially in the younger stages, the evolutionary record is only recoverable from the Pleistocene and Holocene talus relicts (talus flatirons) located at various distances from the remaining relief (Sancho et al. 1988; Gutiérrez et al. 2010, 2015; Peña-Monné et al. 2019, among others). The talus flatiron enables rates for upper scarp retreat to be established (Boroda et al. 2014; Oh et al. 2019). This type of landscape evolution is

This article is part of a Topical Collection in Environmental Earth Sciences on Earth Surface Processes and Environment in a Changing World: Sustainability, Climate Change and Society, guest edited by Alberto Gomes, Horácio García, Alejandro Gomez, Helder I. Chaminé.

✉ José Luis Peña-Monné
jlpena@unizar.es

[1] Dpto. de Geografía y Ordenación del Territorio and IUCA, Universidad de Zaragoza, Pedro Cerbuna 12, 50009 Zaragoza, Spain

[2] Laboratorio de Geoarqueología, Universidad Nacional de Tucumán-CONICET, San Miguel de Tucuman, Argentina

[3] Dpto. de Ciencias de la Antigüedad and IUCA, Universidad de Zaragoza, Zaragoza, Spain

usually recorded in drylands given the alternation of different environmental periods (Gerson and Grossman 1987; Schmidt 1994; Gutiérrez et al. 2010; Sheeland and Ward 2018; Peña-Monné et al. 2019). There are also dissymmetric talus relict developments related to insolation exposure, especially on Holocene slopes (Gutiérrez and Peña Monné 1998; Peña Monné et al. 1996), although this dissymmetry may also have structural explanations (Oh et al. 2019).

The aim of this study was to obtain an evolutionary model and make a palaeoenvironmental interpretation of the residual hills (locally called *tozales)* in the central Ebro Depression (Fig. 1). The environmental cycles are represented by the aggradational and degradative processes in the slopes (talus flatirons) that created the present arrangement of talus flatiron rings. To accomplish this, several hills that are representative of the process were selected and studied using images obtained from sUAV and structure from motion (sfm) photogrammetry. The production of high-resolution geomorphological maps offers exceptional opportunities to obtain detailed information about these landscapes (Hackney and Clayton 2015; Jorayev et al. 2016). Anthropic features provide chronological and geoarchaeological evidence in several evolutionary stages.

Geological and geomorphological settings

Jubierre is located in the central sector of the Ebro basin (Fig. 1). This tectonic depression is filled with continental sediments that accumulated during the Paleogene and Miocene. Paleogeographically, Jubierre is part of the distal section of the 'Huesca alluvial fans' (Hirst and Nichols 1986) coming from the Pyrenees—Alcubierre Fm (Quirantes 1978)—which belong to the Miocene from the Agenian (23.8–20 Ma) to the Vallesian (11.6–9 Ma) (Pérez-Rivarés et al. 2003; Pardo et al. 2004). These fans include the T5 to T7 tectosedimentary units (UTS) of the sedimentary fill of the Ebro basin (Pardo et al. 2004) and are slightly dipped (< 5ºS) and fractured.

In this region, the Alcanadre and Flumen rivers' (Fig. 1) drain, a large surface area of the Pre-Pyrenees and the north side of the Alcubierre mountains. This drainage has produced the wide erosive depression of Sariñena (Fig. 1) on the soft Miocene sediments. The northern sector of the basin is occupied by the fluvial terraces of both rivers, while the southern sector, in the Jubierre area, exhibits a stepped relief of the Miocene limestones (460–480 m a.s.l.) of the Sierra de Alcubierre up to the fluvial channel of the Alcanadre

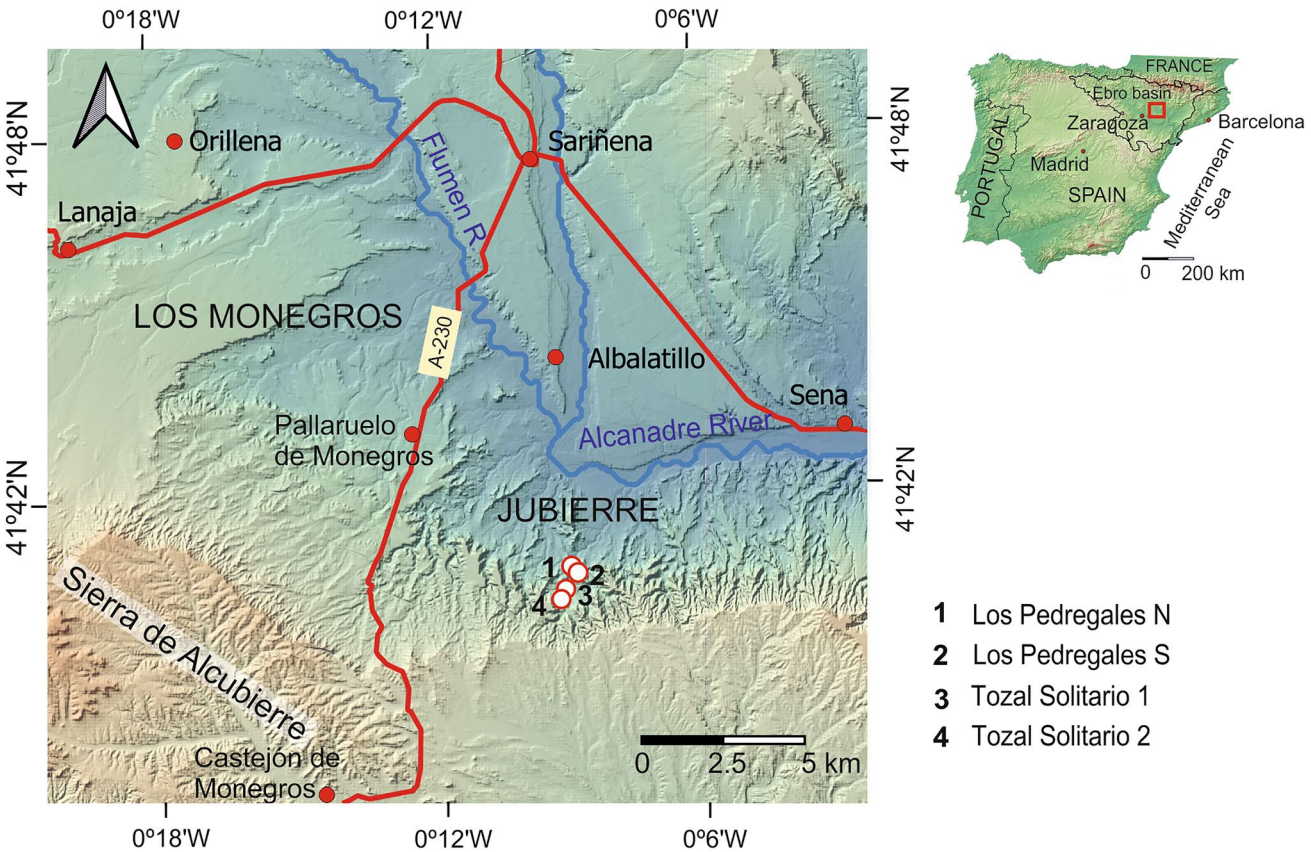

Fig. 1 Map showing the location of the Jubierre area, in the central sector of the Ebro depression, and the hills (*tozales*) analysed

River (224 m a.s.l.) (Fig. 2). In the south, the upper cornice of the Jubierre sector is formed by limestones, marls, and clays from the Sierra de Pallaruelo-Monte de Sora Unit (Ramírez and Solá Subiranas 1990) (Fig. 3a). At the foot of these resistant reliefs are other Miocene units composed of marls, siltstones, variously coloured lutites with interbedded sand channels, and lacustrine limestones and marl layers. They all appear highly eroded (Figs. 3b–e). The Quaternary evolution of the Jubierre piedmont is characterised by the formation of pediments produced by successive Pleistocene aggradation and incision phases whose relicts are also included in the present landscape (Fig. 2).

The current climate is continental Mediterranean with semiarid characteristics; annual average precipitation is 470 mm (Sariñena station) with most precipitation falling in spring and autumn (Cuadrat et al. 2007). The mean annual temperature is around 15 ºC and the area has a significant annual water deficit (-826 mm) that produces a low percentage (~25%) of perennial plant coverage. Vegetation is characterised by open forests of quejigos (*Quercus faginea*), holm oak (*Quercus ilex*), sabin juniper (*Juniperus thurifera*), and pine (*Pinus halepensis*), accompanied by scrubs such as rosemary (*Rosmarinus officinalis*), thyme (*Thymus vulgaris*), and sage (*Salvia lavandulifolia*). Because the valley bottom

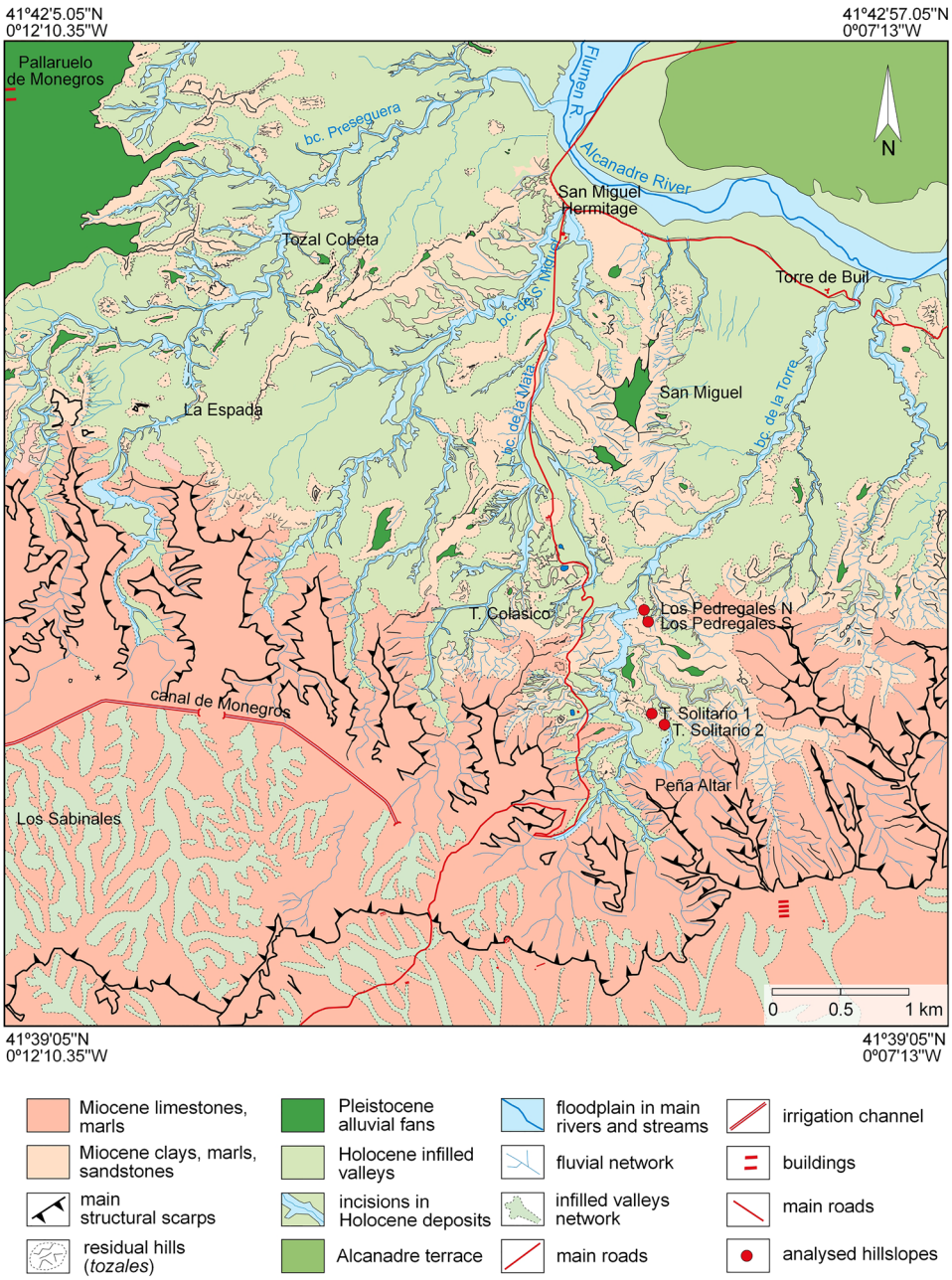

Fig. 2 Geomorphological and geological map of the Jubierre area

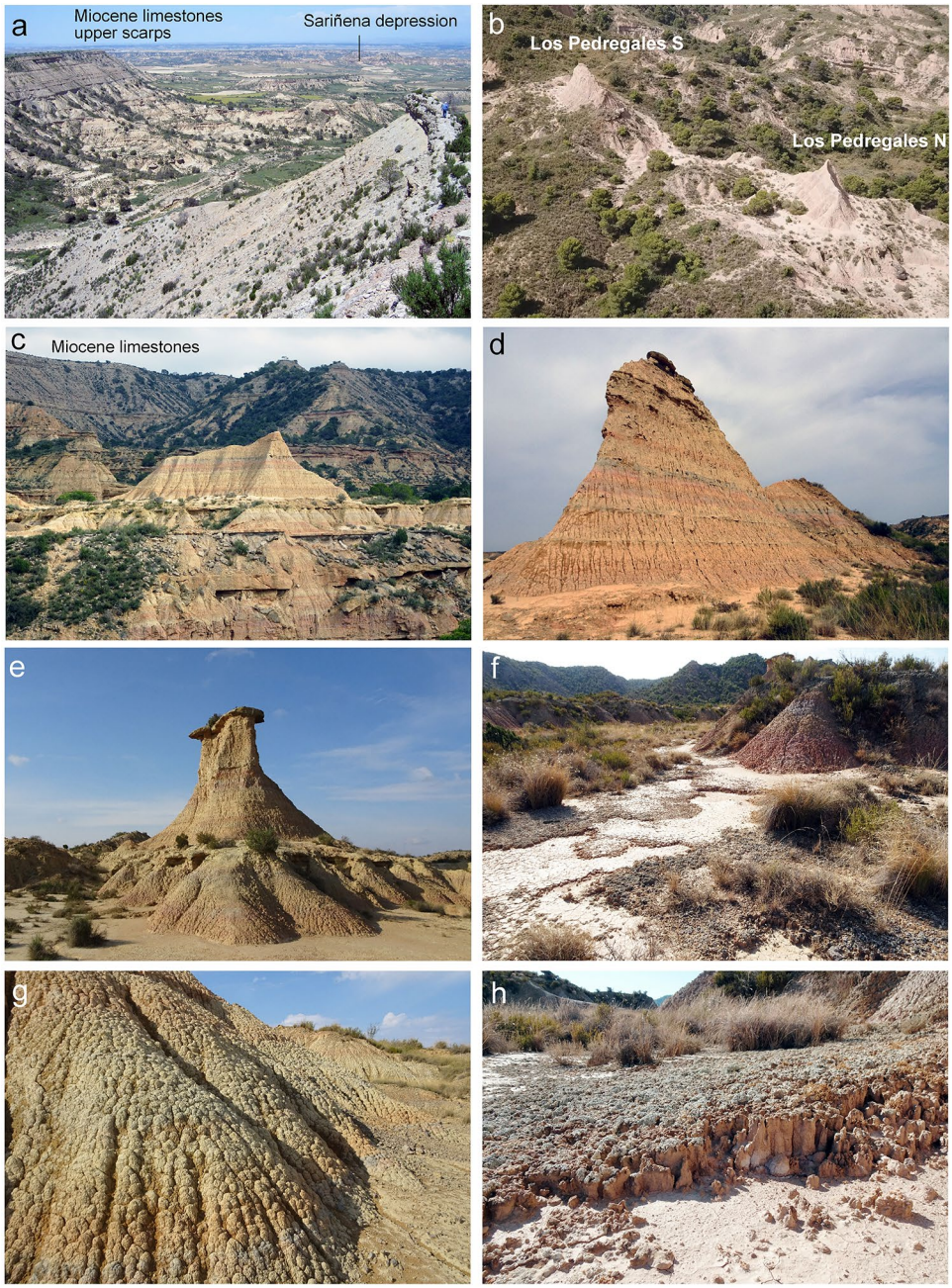

Fig. 3 Images of the Jubierre area at different scales: **a** valleys descending from the upper limestone scarps of Jubierre; **b** aerial view of the residual hills of Los Pedregales; **c** stratigraphy of Sierra de Pallaruelo-Monte de Sora Fm on LPN hill; **d** coloured marls and clays of the LPS hill; **e** Solitario 1 hill; **f** silty alluvial fans at the foot of the hills, arranged as steps and having superficial cracking and biological soil crusts; **g** detail of popcorns and rills developed on clays and marls; **h** soil crusts on erosion processes with pedestal morphologies

soils are rich in sodium, albardín (*Lygeum spartium*) and tamarisk (*Tamarix africana* and *Tamarix gallica*) are abundant near ephemeral water courses.

Methodology

A detailed pedestrian terrain survey of the Jubierre area was made by locating several isolated buttes with adequate orientation and characteristics for the study of slope successions. The selected hills selected showed the most complete sedimentary records, including archaeological information for relative chronological and geoarchaeological purposes. Geomorphological maps were made from spatial datasets (orthoimage and DEM) derived from SfM photogrammetry. Direct field observations were recorded on a Samsung Tab S2 tablet using the QField application for QGIS. Low-altitude (60 m) vertical aerial photographs were taken using the sUAV DJI Phantom 4 with a FC220 camera (12.4 Mpx) controlled by a remote controller supporting an Android mobile device. The flight was preconfigured with Pix4D-Capture, and 286 photographs (80% overlapped) were taken in two perpendicular grids to improve accuracy and covering an area of 0.138 km^2. The pictures were processed in

Agisoft Metashape Professional v.1.5.1 to obtain an orthomosaic with 2.36 cm/pix ground resolution and a DEM with a 4.72 cm/pix resolution. The DEM was transformed into contour lines, topographic profiles, and a hill-shaded model to enhance the terrain features and estimate the position of landforms to improve mapping.

Highly detailed geomorphological maps from the two selected hills (Los Pedregales N and S) were digitised at 1:468 scale in QGIS v.3.12.2, following the legend proposed by Peña Monné (1997). The detail was necessary due to the dimensions of the hills, surface textures, and the need to highlight the erosive and accumulative landforms. The detailed topographic cross-sections made from the DEM were used for measuring the features related to landscape morphological evolution, and these were traced across the slopes corresponding to all evolutionary stages. Two other hills, Solitario1 and Solitario 2, were synthetically studied to complete the information about older stages. Slope and talus flatiron gradients were determined with a clinometer.

Each butte was intensively surveyed by full coverage. Taking the butte as a starting point, 1-m-spaced concentric circles were walked in search of archaeological evidence. Potsherd sets related to different taluses were recovered and ceramic fragments were used to estimate slope deposit chronologies and their potential provenance, as well as the connections among the taluses.

At Los Pedregales S, a 1-m-wide front of the talus was cleaned to establish the stratigraphic sequence. One charcoal sample representative from this outcrop was dated by ^{14}C AMS by DirectAMS Laboratory (USA). Potsherds were classified and morphometrically and technologically described following the proposal of Picazo (1993) for Bronze Age fragments. The technological study of ceramic pastes followed the usual procedures (cfr. Orton et al. 1993) with an emphasis on inclusions (proportion, shape, and type) and was made by macroscopic observation followed by microscopic analysis with a 50 × digital Dino Lite.

Results

The Alcanadre River has its head in the Pyrenean External Ranges and reaches the Sariñena depression with a N-S orientation. At the confluence with the Flumen River, it turns 90º towards the east (Fig. 1) to finally merge with the Cinca River. The Alcanadre River migrates to the south along the Middle/Upper Pleistocene and constitutes a boundary between the smooth relief of the large Quaternary deposits of Sariñena to the north and the abrupt and geomorphologically diverse reliefs of Jubierre to the south. The ephemeral streams coming from the upper limestone reliefs south of the Jubierre descend around 250 m to join the Alcanadre River (Fig. 2). These streams show an average gradient of 5–6%. Their strong erosive power has led to the headward erosion of the basin (Fig. 3a).

There are several levels of Quaternary pediments on the south margin of the Alcanadre River (Fig. 2). They form narrow morphologies that divide the valleys where the main streams flow. These pediments are residual landforms of a large detritic cover and form slightly tilted mesas and testimonial buttes (Fig. 2). The escarpment rim is mainly formed by accumulations of angular limestone fragments coming from the cornices of the Sierra de Pallaruelo-Monte de Sora Unit. These accumulations developed in several stages and represent periods when high loads were carried by streams from Jubierre and formed large detritic mantles along the piedmont. At present, incision processes affecting the entire piedmont are dominant and expose the erodible subjacent marls and clays (Figs. 2, 3c). It is sometimes possible to find interbedded resistant layers (sandstones and limestones) in the form of narrow steps with segmented scarps and buttes (Fig. 3d, e). Where the resistant layers are eroded, there are only residual hills following a long evolutionary process. The result is a complex labyrinthine landscape with almost no human activity, conferring great scenographic value to the area.

Many residual hills (*tozales*) are currently very unstable due to erosion caused by several factors. First, their morphology is very abrupt, with slope gradients over 60º. The lack of hard layers on the top of the morphologies and the scarce vegetation cover create a wetting front exposed to rain splash (Fig. 3c–e). In addition, the hills develop a steep hydraulic gradient with respect to the drainage base level of the surrounding streams, and this leads to high flows with considerable carrying capacity. Second, the lithologies are prone to erosion as they are composed of lutites and marls with a high level of calcium and sodium sulphates. Lastly, the present semiarid climate is characterised by scattered concentrated rains (with events reaching up to 60–80 mm/24 h), and especially convective storms during the summer which magnify the factors previously mentioned.

The rill subparallel networks are developed from the upper middle sector of the hills (Fig. 3d) with popcorn interills in the lower sections of the hillslope. When intermediate steps are present, it is possible to find conical forms (locally known as 'elephant legs') with gullies and pipes (Fig. 3f, g). These surfaces tend to be covered with popcorn morphologies and pedestals (Fig. 3g), and sometimes with large amounts of saline efflorescence. Much of the water flows through piping to reach flat surfaces, such as the structural landings at the base of the hills. Sediment movement reaches a high level of efficiency by developing silty alluvial fans in the piping outlets as well as surface runoff (Fig. 3f). These environments change quickly and give rise to various stages of stepped micro-alluvial fans formed by silty sediments moving through incision cycles. High levels of polygonal

cracking density are usually found on these silty-clay accumulations. These cracks facilitate rain penetration until they are sealed by sediments or biological soil crusts (Fig. 3h). Biological crusts are formed by lichens and mosses and can temporally slow erosion. These morphologies are shown on the map of Los Pedregales when they are large enough to be represented on our working scale.

We will now focus on the evolutionary study of the slopes of two of the most geomorphologically interesting hills: Tozales of Los Pedregales North (LPN) and South (LPS) (Fig. 3b–d). These two hills are in the central sector of Jubierre. Both were formed on the detritic sediments of the Bujaraloz-Sariñena Fm of Agenian-Aragonian age. They are composed of marls, clays, and siltstones (red, orange, and yellowish). Some narrow layers of lacustrine limestones and sandstones generate largely resistant steps among the soft sediments (Fig. 3c–e). There are also some greyish sandstone palaeochannels on the lower section of the accumulations found at the stream incisions, like in the Barranco de la Torre (Figs. 2, 3c). Both hills are located over narrow platforms, the LPS being higher than the LPN (Fig. 4a). These platforms are surrounded by deep incisions produced by the fluvial network. The hills are N-S oriented and clearly visible in the landscape due to their topography and lack of vegetation (Fig. 3b–d). Each hill is surrounded by a set of talus flatirons formed by accumulations of angular limestone gravels and blocks containing information about the Quaternary evolution. Some talus flatirons also contain archaeological remains of interest for the reconstruction of human settlements.

Los Pedregales North (LPN)

The LPN hill has an elongated NNE-SSW shape with a central crest that lacks a resistant upper caprock, so it can be classified as a residual hill. It is 25 m long and 12 m wide and composed of marls and clays with interbedded thin limestone layers. The water divide is formed by a sharp crest with 255 m a.s.l. to the SSW and 252 m a.s.l. to the NNE (Figs. 3c, 4a, b). The hilltop is 8 m above the structural platform over which it is located and 27 m above the Barranco de la Torre stream channel. The geomorphological map (Fig. 5) shows the isolated position of the hill lying on the flat structural surface and the narrow steps formed by limestone and sandstone descending towards the stream channel. The permanence of the present hill depends on the hardness of these basal structural levels (Figs. 5, 6a, b). The main scarp is N-S aligned, and its retreat has produced many large blocks that cover part of the slope.

The LPN hill is characterised by the strong erosion caused by microrills and micropiping created by runoff and epidermal flows (Fig. 5). The stony compositions of

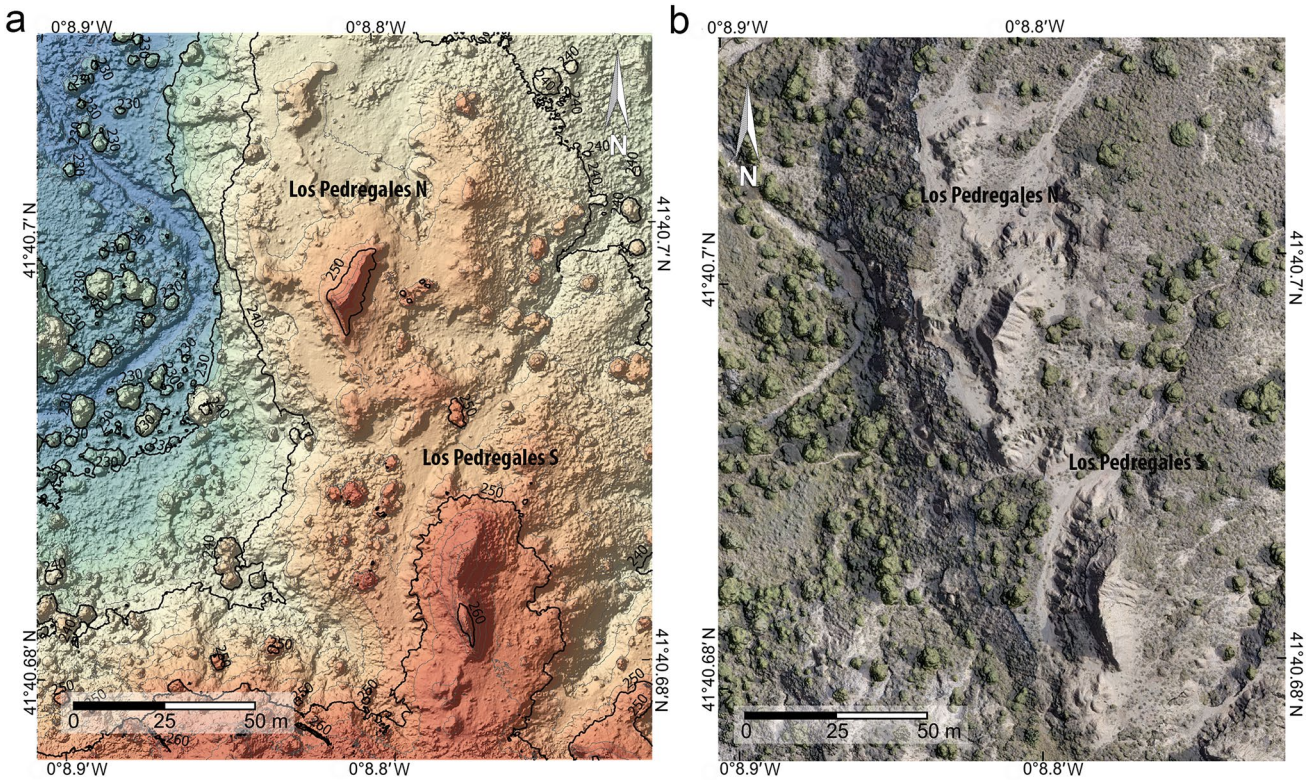

Fig. 4 DEM and orthoimage obtained from UAV flights for LPN and LPS

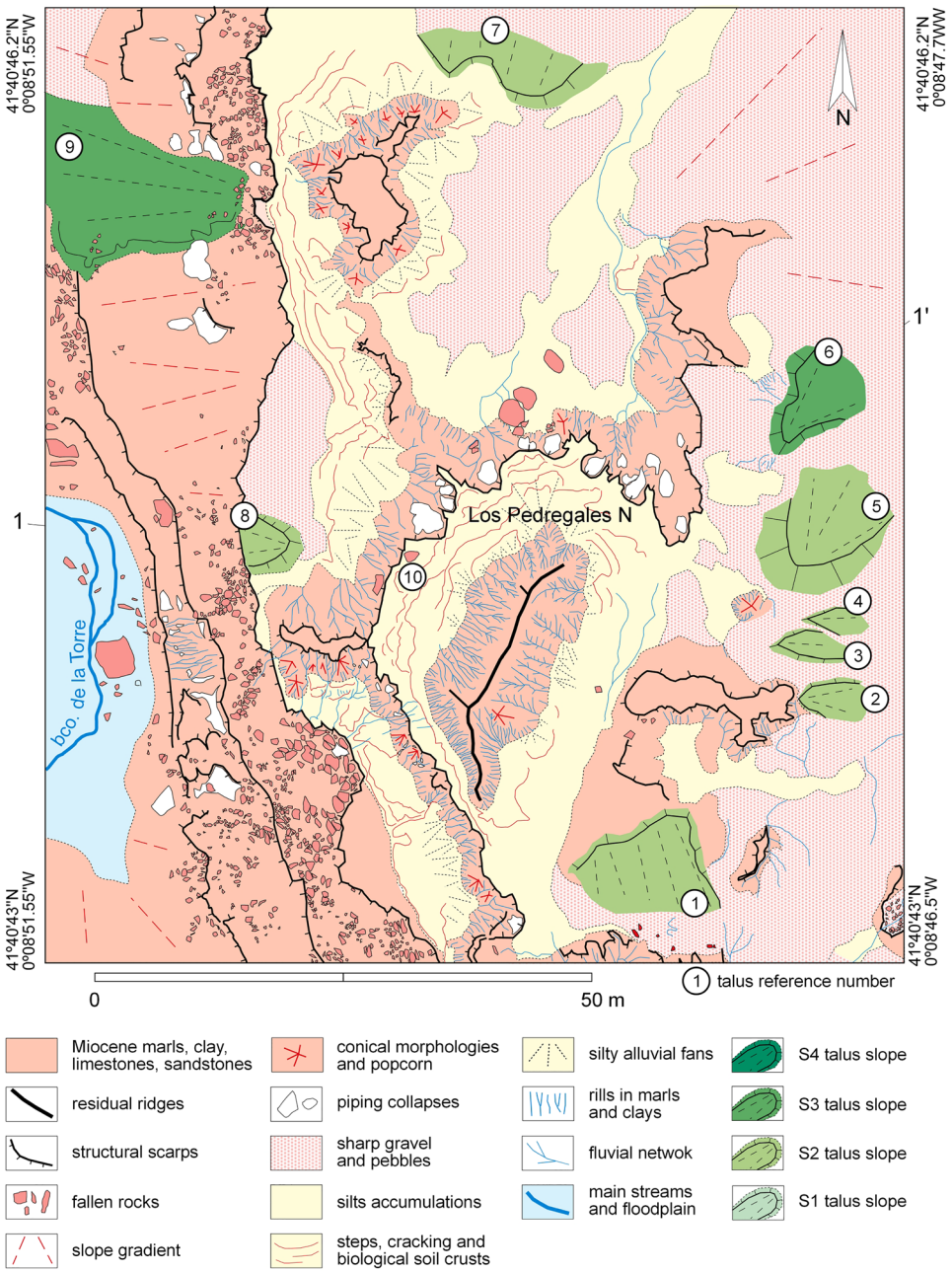

Fig. 5 Detailed geomorphological map of LPN hill and general references. Marginal numbers indicate the cross-section of Fig. 6b

the residual slopes mean that have been preserved. Their reliefs have subtriangular shapes, typical of talus flatirons, and feature a high sharpened apex and a smooth reverse (Fig. 5). The deposits are formed by angular limestone heterometric clasts (pebbles to blocks). Two sets of taluses of different ages were identified and classified according to their distances from the LPN hill and height, as well as the presence (or absence) of archaeological remains. After all the recorded hills from Jubierre were classified, the furthest and, therefore, oldest slopes from LPN are listed as S3 and their remains are named taluses 6 and 9 in Fig. 5 (see also Fig. 6a). No archaeological remains were found for this stage. The next stage, S2, is younger and closer to the hill than the previous stage (S3) and is mainly preserved towards the east of the hill (taluses 1 to 5 in Fig. 5) (see also Fig. 6a, b). There is also a small relict of S2 on the border of the western scarp (talus 8 in Figs. 5, 6a) and another considerably eroded relict towards the north (talus 7 in Fig. 5).

Most S2 taluses reveal ceramic Bronze Age potsherds—rolled by transport—among the limestone clasts (Fig. 6a, c, d). Eighteen ceramic fragments and several flints were recovered from talus 1 (Fig. 5). There are also fragments of mud bricks and mud pavement fragments on taluses 3 and 5, although the quantity was small and the chronological

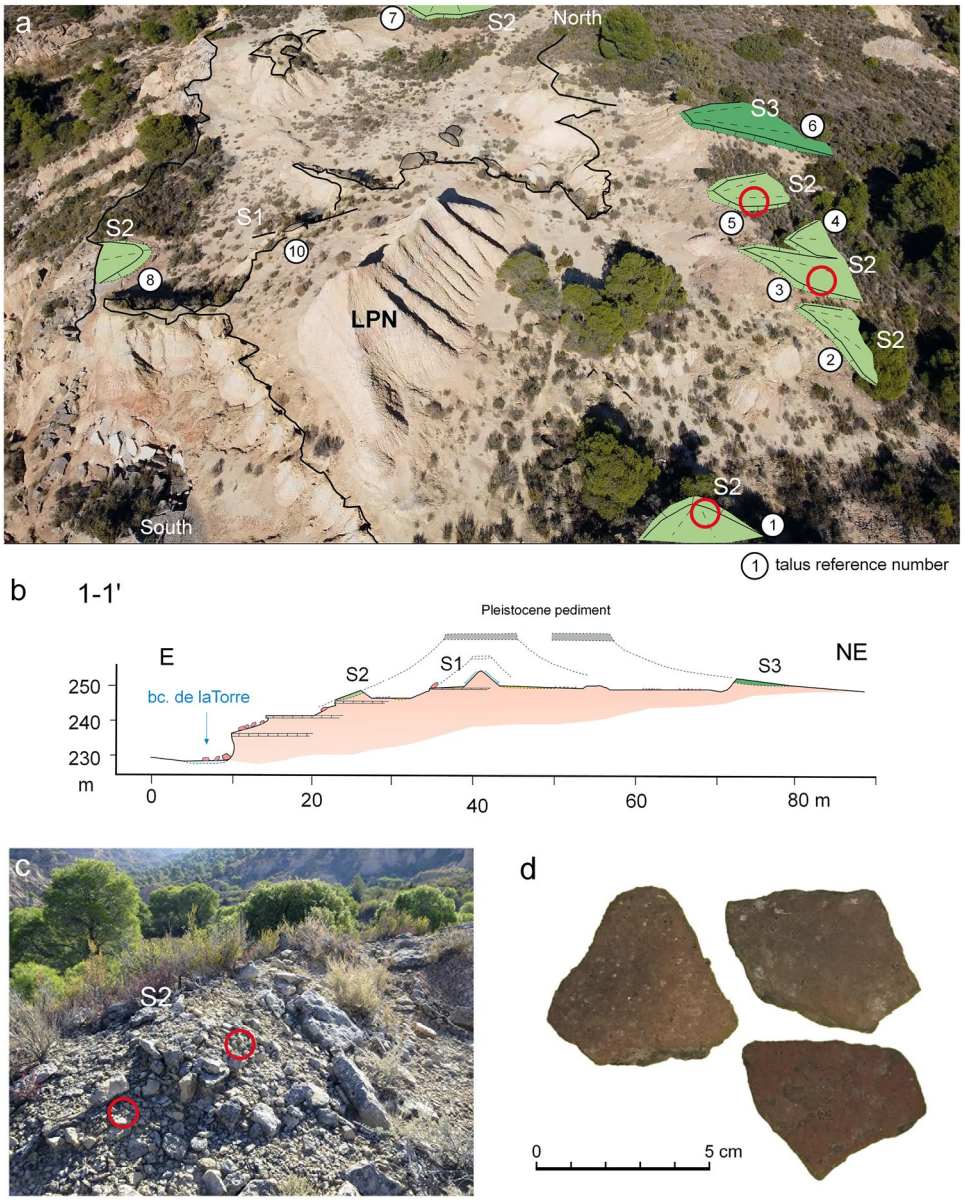

Fig. 6 **a** General aerial view of LPN hill and the S2 and S3 talus flatirons set; **b** and cross-section showing the arrangement of the different slope stages; **c** location of several Bronze Age potsherds on S2 talus; **d** detail of three ceramic fragments interbedded in S2 stage

value low. The ceramic fragments recovered from talus 1 belong to small vessels made with a fine paste. They were part of open carinated vessels that are typical of the intermediate and late phases of the Bronze Age (second millennia BC; Picazo 1993). A distal section of a flint laminate fits within the proposed chronology.

In addition, it was possible to observe severely weathered sandstone blocks, some of which are large, sparse, and isolated. These blocks must have been part of the hill caprock at an intermediate phase of its evolution. One of these blocks remains in an inclined position on the slope deposits. Because of its proximity to the hill, this block is part of the only remains of the S1 stage. It is represented in Fig. 6a (number 10) and on the profile of Fig. 6b.

Los Pedregales South (LPS)

LPS is located on a structural platform above the base of LPN. The hill is 37 m long and 12 m wide, reaching 14 m in height at 262 m a.s.l. and is located 34 m above the Barranco de la Torre channel (Fig. 4a, b). It is separated from LPN by a pass (through which much water drains towards the NE) (Fig. 7a). It is geomorphologically more complex than LPN, and in the southern sector, it still includes part of a 30-cm-thick protective sandstone caprock (Fig. 3d). After a small pass, the hill extends towards the NNE as a descending crest with narrow remains of the S2 stage (talus 8 in Fig. 7a–c). The slope has a steep gradient, because it is close to the Barranco de la Torre.

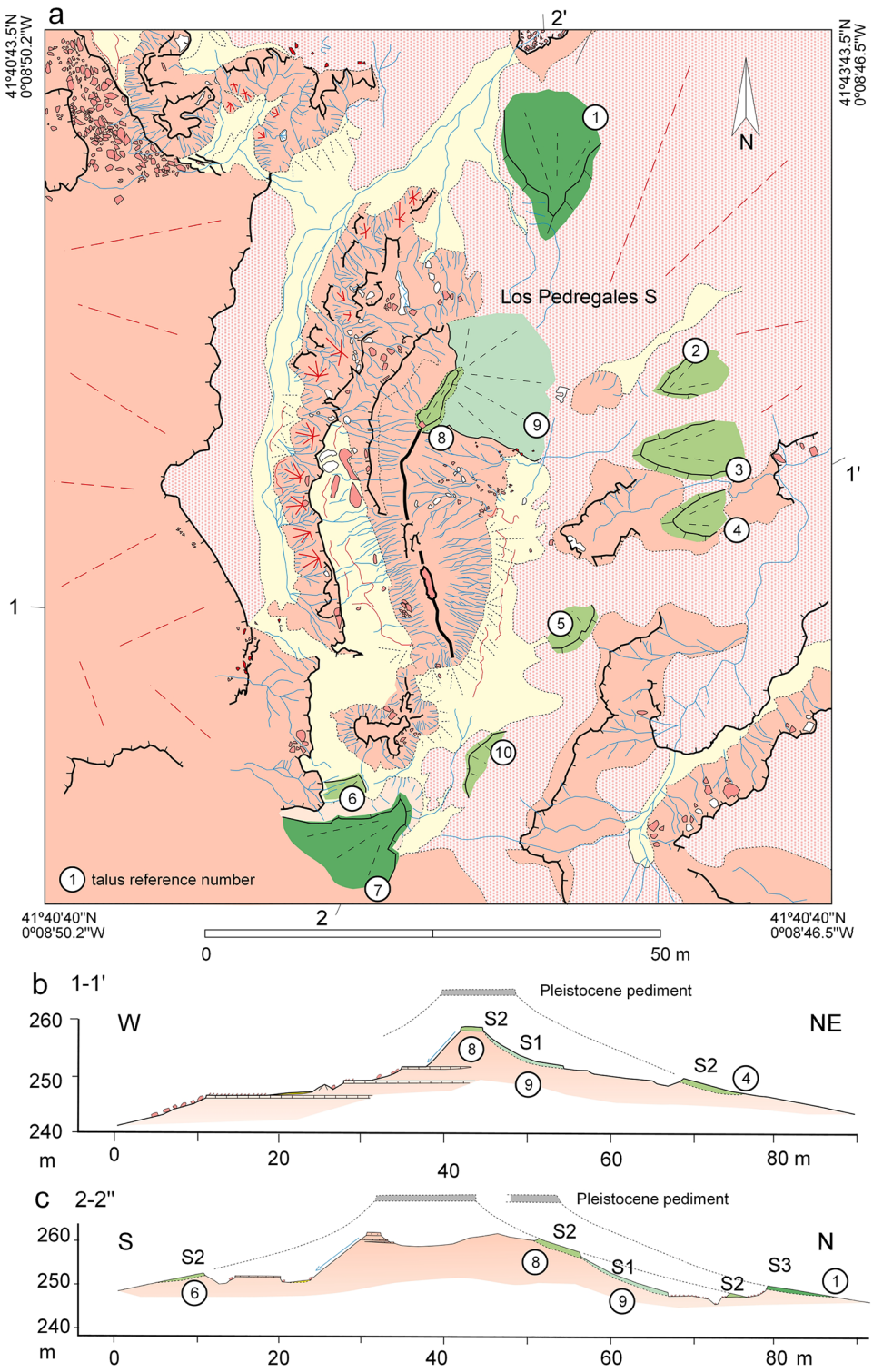

Fig. 7 **a** Detailed geomorphological map of the LPS hill. References are the same as in Fig. 5. Marginal numbers indicate the cross-section locations; **b**, **c** cross-sections of LPS hill showing the talus flatirons stages

It has a stepped appearance, because it developed over the sandstone and limestone scarps descending towards the stream channel. It is possible to find clay and marl micromodelling around the steps produced by rills and piping (Fig. 7a). There are cones, popcorns, vertical mood covers, and micro-pedestals among the piping outlets. Like on the LPN, clay layers without hard protection are exposed on the LPS. The layers are affected by a dense network of microrills and piping (Fig. 7a) with the formation of silty cones at the foot (Fig. 3f). The hill also shows step formations and surficial processes of cracking and biological soil crusts (especially towards the south).

There are remains of older slopes with talus flatiron morphologies. Three evolutionary stages were identified. Two triangular shapes with the apex oriented towards the hill are from the older (S3) stage (taluses 1 and 7 in Figs. 7a, c, 8a). These shapes have a 0.3–0.4-m-thick deposit on the apexes that decrease along the backslope and are composed of angular limestones from the Jubierre—without any material with chronological meaning.

Stage S2 is represented by four very eroded taluses located on the eastern side of the LPS hill (Figs. 7a–c, 8a)

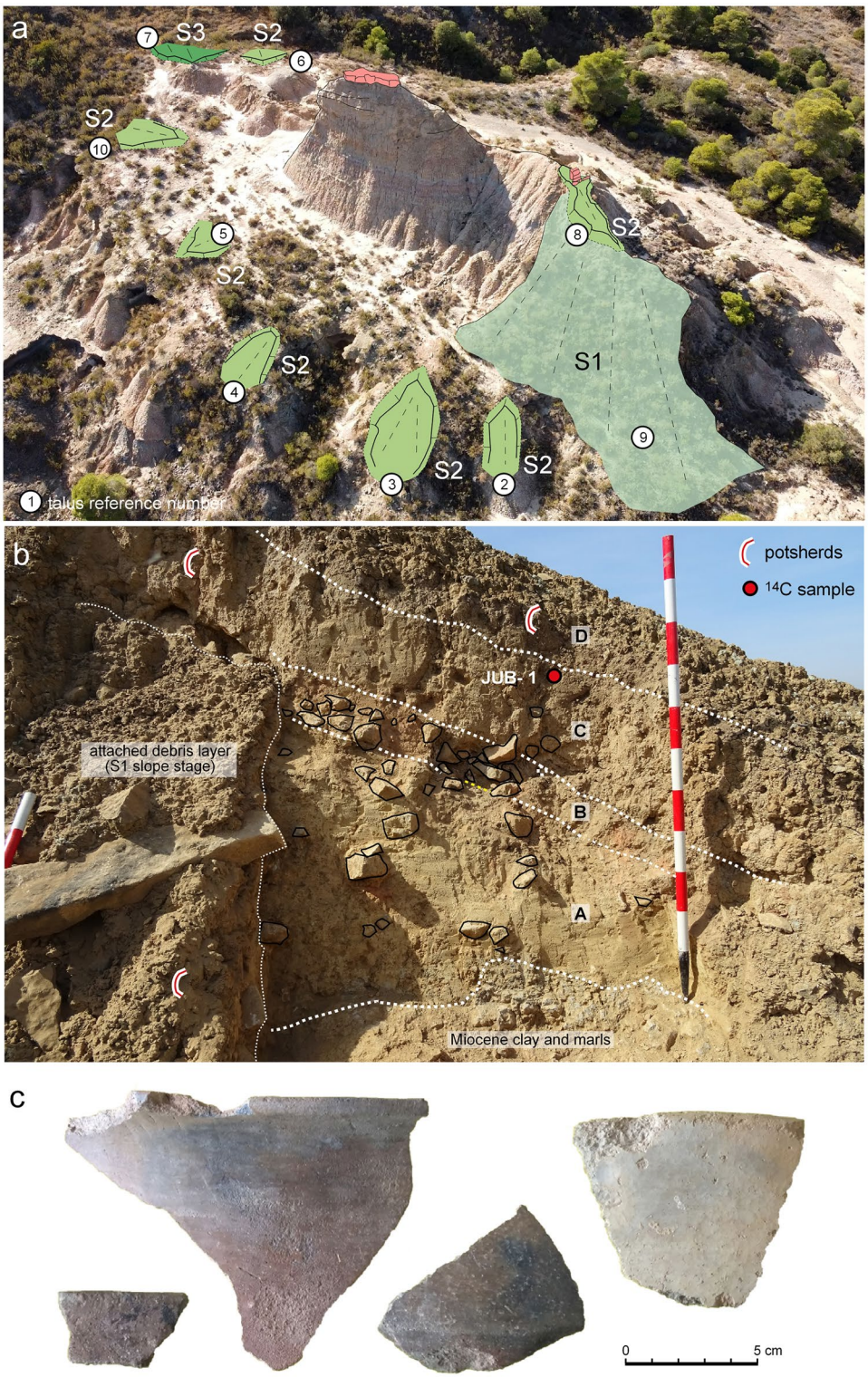

Fig. 8 **a** Aerial view of LPS with preserved talus slope; **b** S2 outcrop after archaeological inspection and clearing with layers indicated, location of the ^{14}C sample and potsherds; **c** Bronze Age potsherds from S2 talus

with talus remains to the SW (Fig. 7a) on the side of the main scarp (Fig. 7c). There were probably other remains of the same stage towards the west, but these were eroded due to their proximity to the Barranco de la Torre. One of the taluses (talus 5 in Fig. 7a) is oriented in the opposite direction to the rest of the arrangement and probably belonged to another relief located towards the SE. Most eastern slopes from stage S2 (taluses 2, 3, 5, and 10 in Figs. 7a, 8a) have ceramic Bronze Age potsherds (the same stage as in LPN) and limestone detritic deposits.

The most outstanding S2 talus is located to the north of the hill crest (talus 8 in Figs. 7a, 8a) and is exceptionally well preserved in the middle section of the butte. This is because there are many sandstone blocks on its apex protecting an S2 slope with a thick and compact deposit. The development of a biological crust also improved its resistance. The most recent slope (S1) is located on the eastern foot of the hill (talus 9 in Figs. 7a, c, 8a) and partially lies on an escarpment wall that also contributes to its conservation.

Considering the abundance of ceramic fragments, bones, and charcoals in the S2 (8) relict, a 1-m-wide segment of the middle section of the outcrop was cleaned and described (Fig. 8b). The clayey sediments with blocks covering the S2 escarpment and the head of the S1 slope were removed to access the S2 deposit. Although this is not a primary archaeological site, such removal is the best approach to learn about the human occupation of the hill over the ages.

The S2 deposit lies on the clays and marls of the Miocene substrate (Fig. 8b). The deposit reaches 120 cm in thickness and diminishes downslope to 80 cm in thickness to the left (S) diminishes downslope to 80 cm in thickness. The first unit (A) is composed of yellowish clays with limestone clasts chaotically distributed, whose major axes range between 2 and 10 cm. The unit also contains charcoal fragments. It is followed by Unit B, which slopes 26º and cuts through the previous unit. Unit B is about 20 cm thick and composed of reddish clayey sediments with limestone clasts arranged along the inclination of the slope (Fig. 8b). It is a very continuous unit located below the base of the talus. Unit C is 20 cm thick, formed by yellowish silty sediments with the same inclination as the previous unit. It contains bone and charcoal but no ceramic fragments. A charcoal sample was taken (JUB-1) at a 30-cm depth close to the contact with the upper unit (D) (Fig. 8b) and dated to 3252 ± 24 BP (1608–1446 cal BC, 2σ) (Table 1). Lastly, Unit D is formed by 20 cm of greyish silts that are completely grey on the top. The surface is covered with an eroded biological crust. Ceramic fragments are more abundant on this upper unit than in the rest of the profile.

The archaeological survey and excavation made on slope 8 of the S2 stage provided ceramic fragments and lithics that resemble those of the S1 slope located at its foot (talus 9 in Figs. 7a, 8a). The ceramic fragments of S1 are the result of the erosion and sedimentation of the upper S2 slope. The ceramics are generally well preserved and show sharp edges, unaltered surfaces, and rounded shapes. In addition, a flint flake with thermal cones, a firing pin made of a fluvial quartzite, and bone and charcoal fragments were recovered.

The ceramic set is composed of eight fragments of hand-modelled Bronze Age vessels, which were especially common in the middle and late phases. Chronologically, they are dated between 1700 and 1000 cal BC, following comparison with other regional studies (Picazo 2005). Noteworthy features are the open edges (Fig. 8c) corresponding to medium-sized and small vessels with carinated or S-shaped profiles, burnished finishes, and fairly good-quality pastes. There are three main paste compositions: (i) mostly chamotte; (ii) mostly quartz; and (iii) mostly mica and quartz. The same materials were recovered from all the taluses showing chronological connections.

Other slopes from the S2 stage arranged as talus flatirons also contain ceramic potsherds, such as taluses 3 and 5 (Figs. 7a, 8a). These are smaller and rounded due to the distance from the main hill. They also have the same paste composition and typologies as those found on taluses 8, 9, (Figs. 7a, 8a) and the LPN taluses.

The younger S1 stage (talus 9 in Figs. 7a, 8a) is found at the foot of the remains of S2 and contains the materials eroded from the previous stage. The surface of S1 has a stony appearance due to the erosion of fine sediments, but the deposit contains abundant silt and clay, together with ceramic fragments, like in S2. The preservation of the S1 slope may be related to the protection provided by the upper S2 remains, although in the past, it must have covered the entire middle slope and foot of the hill.

The slopes in other residual hills

There are many residual hills with talus slopes in this region, and there is a lack of chronological information for some of these hills. Information from two hills from other region with well-preserved slopes and including old stages (S3, S4)

Table 1 Radiocarbon datings

Sample	Lab code	Age yr BP	Age cal BP		Age cal BC/AD		Sampled material
			1 σ	2 σ	1 σ	2 σ	
JUB-1	D-AMS 041195	3252 ± 24	3484–3410	3557–3395	2535–1461 BC	1608–1446 BC	Charcoal

were found and used to complete the general evolutionary model. Both hills (Tozal Solitario 1 and Tozal Solitario 2) are very close to LPN and LPS and have similar lithological and geomorphological characteristics, although their final morphologies differ.

Solitario 1 is N-S oriented and retains a sandstone layer in the south sector (Fig. 9a, b), while the middle to northern area is a narrow clayey crest falling to the north. This hill presents old slopes from past stages (S4 and S3) that are especially large on the west side (Fig. 9a, b). As in LPN and LPS, a Bronze Age potsherd was found (Fig. 9d) among the limestone clasts of slope S2 (Fig. 9c).

Solitario 2 is a clayey hill with a sandstone caprock that completely lacks vegetation. The hill is deeply cut by rills and piping located above a thick sandstone platform on which the cones of silt and gravels carried by the rills descending from the hill wall are deposited (Fig. 10a). Two S3 slopes are preserved while the S2 talus ring is completely preserved except towards the eastern hill face (Fig. 10a, b). Three large ceramic fragments, perhaps belonging to the same vase, were found at one of the talus flatirons of the S2 stage (Fig. 10a, c). These potsherds (Fig. 10d) show thickness, finish, and inclusions similar to those already described belonging to the Bronze Age although they present rounded edges. Solitario 2 also retains a small talus close to the present hill from the S1 stage (Fig. 10a, b).

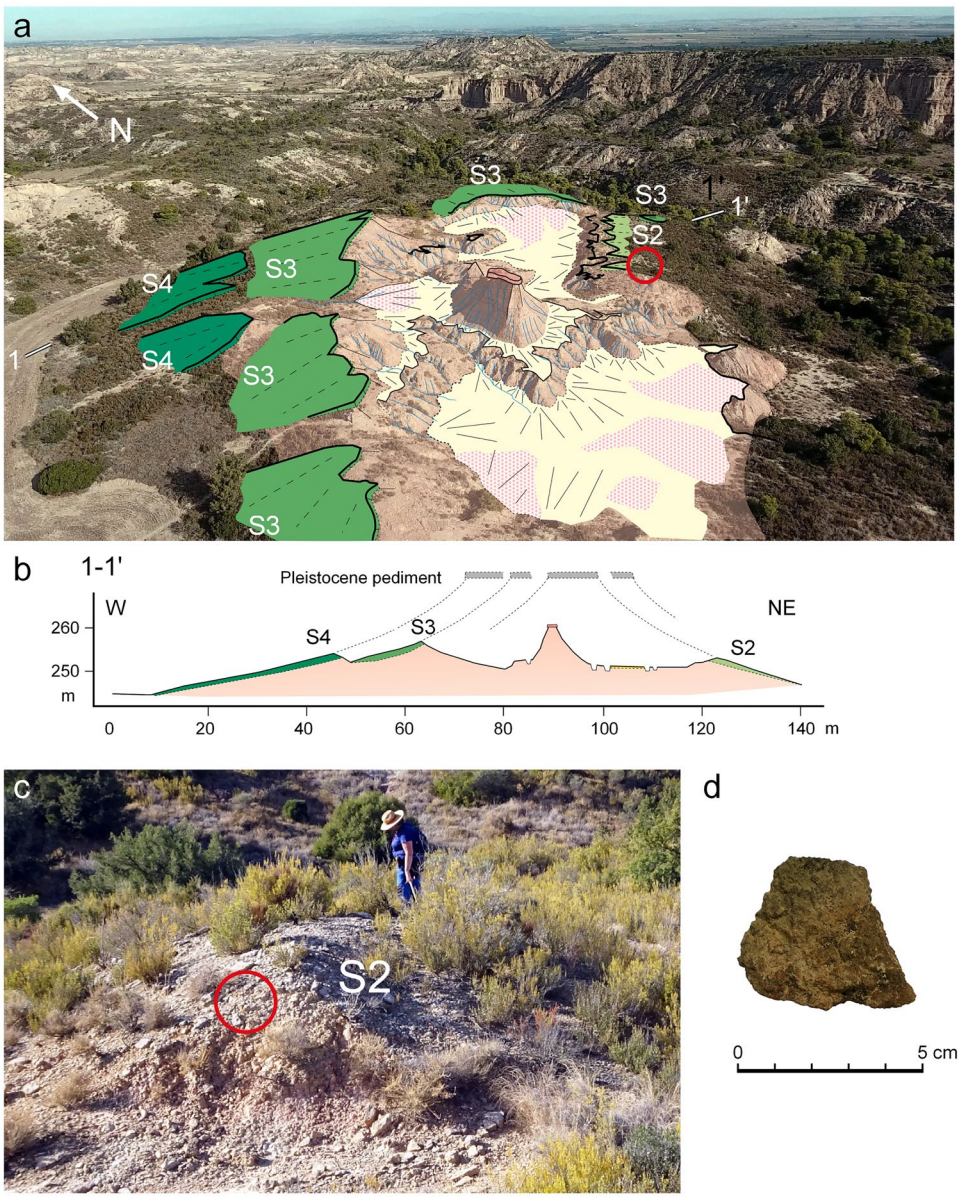

Fig. 9 **a** Geomorphological interpretation of Solitario 1 hill from oblique UVA photograph and location of (**c**) (red circle); **b** cross-section across Solitario 1 hill as indicated in (**a**); **c** talus flatiron S2 and location of the Bronze Age potsherds (red circle), one of them shown on (**d**)

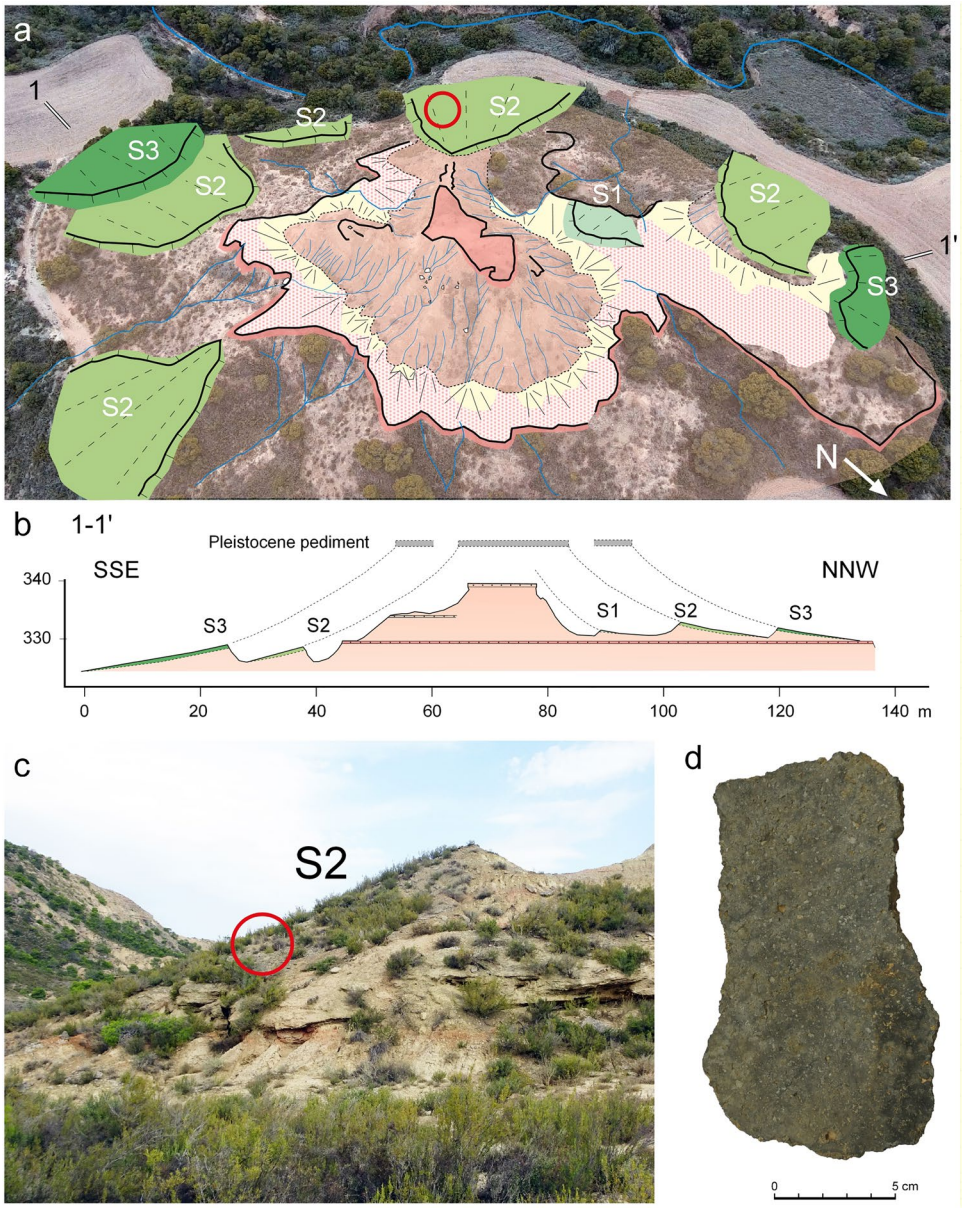

Fig. 10 **a** Geomorphological interpretation of Solitario 2 hill from oblique sUVA photograph and location of (**c**) (red circle); **b** cross-section of Solitario 2 hill as indicated in (**a**); **c** talus flatiron S2 and location of the Bronze Age potsherds (red circle), one of them shown on (**d**)

Discussion

The geomorphological arrangement and hill formation

The four hills analysed have the same lithological composition and are part of the same starting geomorphological arrangement. The lutites and marls of the Bujaraloz-Sariñena and Galocha-Ontiñena units (Agenian-Aragonian) are highly erodible, despite the interbedded sandstones and limestones. At present, piping and runoff (rills and gullies) comprise evidence of high erosion rates for the Miocene materials. Throughout the Quaternary, the Alcanadre River represented the general base level of the drainage network of Jubierre. The fluvial network of Jubierre is formed by steep ephemeral streams flowing in parallel towards the Alcanadre River. The confluence of these streams is perpendicular to the Alcanadre River, because it turns east after merging with the Flumen River (Figs. 1, 2). The aggradational, stabilisation and incision phases of the Alcanadre floodplain determined the aggradative/degradative dynamics of the Jubierre tributaries, resulting in the formation of pediment stages with gradients oriented towards successive Quaternary base levels. Thus, at the beginning of the erosive process, there was a lateral connection between pediments and fluvial terraces.

The detrital cover of the pediments, with thicknesses of 2–6 m, is preserved in the upper section of the numerous reliefs located in the middle and lower sectors of Jubierre (Fig. 2). These reliefs form mesas and residual hills at

various altitudes (Fig. 11) and also form water divides among the water courses deeply entrenched in the soft Miocene materials. Thus, their morphologies are S–N oriented. The arrangement of parallel S–N drainage networks and intermediate reliefs is still present.

The evolutionary process evidenced by the residual slopes is the result of the erosive retreat of the intermediate reliefs in all the margins. This is particularly evident on E and W slopes. These margins are highly dynamic due to the nearness of lateral streams. Therefore, the resulting reliefs are narrow and S–N elongated.

Another important factor is insolation exposure. In our studied cases, slope development does not differ, because we chose subelliptic hills with few slopes oriented in N-S direction. The orientation factor produces notable differences in incident energy and the humidity available to maintain a protective plant cover. Orientation also influences the capacity for recuperation after fire, overgrazing, and other human activities (Burillo et al. 1981; Burillo and Peña Monné 1984). Differences in orientation explain the development of dissymmetric hills (Peña Monné et al. 1996), because erosion is greater on south-facing slopes (Northern Hemisphere). North-facing slopes can be more stable and even insensitive to short-term environmental changes, especially during the Holocene (Peña Monné 2018).

The limestone lithologies of the detritic materials composing the taluses are not present in the Miocene composition of the hills. However, these lithologies are only present on the Pleistocene pediments of Jubierre and the high Miocene limestone corniches of the Sierra de Alcubierre. This enabled us to infer that the original caprock of all the hills was a detrital cover of the pediment. This type of material is currently identifiable in situ in other nearby less eroded hilltops (Fig. 2). These top deposits are cemented by carbonates that have become resistant calcretes (Sancho and Meléndez 1992; Meléndez et al. 2011). These detrital levels are represented in the cross-sections (Figs. 6b, 7b, c; 9b, 10b) of the inferred past positions. Their positions and altitudes were estimated from nearby reliefs that still retain these covers, together with inclined taluses. We estimate that the same pediment level covered LPN, LPS, while Solitario 1 and Solitario 2 were probably covered by a higher and then older pediment.

Many reliefs from Jubierre have Quaternary pediments on their tops, but it is difficult to establish stages because they are small and disconnected from each other (Fig. 2). Four stages were identified in the topographic cross-section (Fig. 11) drawn between the southern limestone platforms (Sierra de Alcubierre) and the Alcanadre River (N), although there are some higher remains. The theoretical surface level was reconstructed through the platform surfaces up to the Alcanadre River as a base level to enable establishing these surfaces at 90–100, 55–60, 30–35, and 10–12 m above the present river channel (Fig. 11). The fluvial terraces of the Alcanadre River in the Sariñena area are located at 180 m (Qt1), 120 m (Qt2), 55 m (Qt3), 30 m (Qt4), 20–25 m (Qt5), 25 m (Qt6), 10 m (Qt7), and 3–5 m (Qt8) above the present channel (Calle et al. 2013). These relative heights enabled us to consider possible relationships between the 90–100 m pediment and Qt2 terrace, that of 55–60 m with Qt3, that of 30–35 m with Qt4 or Qt5, and that of 10–12 m with Qt7. Considering the fluvial terraces of the left margin of the Alcanadre River (no terraces are preserved on the right margin), the most topographically probable pediment related to the LPN, LPS, and Solitario 1 hilltops is that of 30–35 m (Fig. 11), and this could be connected with Qt4 or Qt5 fluvial terraces. The Qt5 was dated by OSL between 196 ± 13 y and 274 ± 18 ky (Rodríguez-Ochoa et al. 2019). The Solitario 2 top may be the pediment connected with Qt3 or Qt4 terraces and older than the other hills. However, this is difficult to establish without direct datings.

In the reconstruction shown in Fig. 12, a pediment is represented as the starting landform for the evolution of these hills without establishing an age. From the progressive retreat of the upper scarp, successive phases of stabilisation or incision were established on the slopes. This process, represented in Fig. 12a–e, was accompanied by the intense incision of the surrounding ephemeral streams as the hills shrank. The detrital caprock loss was sustained up to the S2 stage on the four hills analysed because the eroded materials are found on the S4, S3, and S2 stages. The younger stage (S1) is present in LPS and composed of the materials eroded

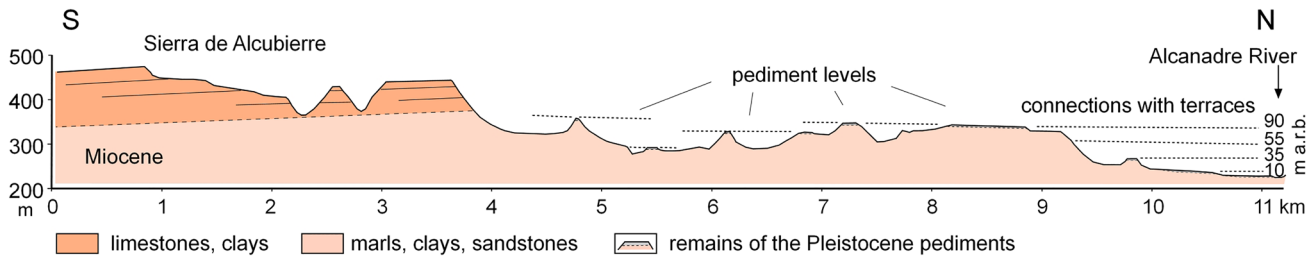

Fig. 11 **a** Topographic cross-section of the Jubierre reliefs from the upper limestone platforms (Sierra de Alcubierre) to the Alcanadre River with the reconstruction of the pediment levels

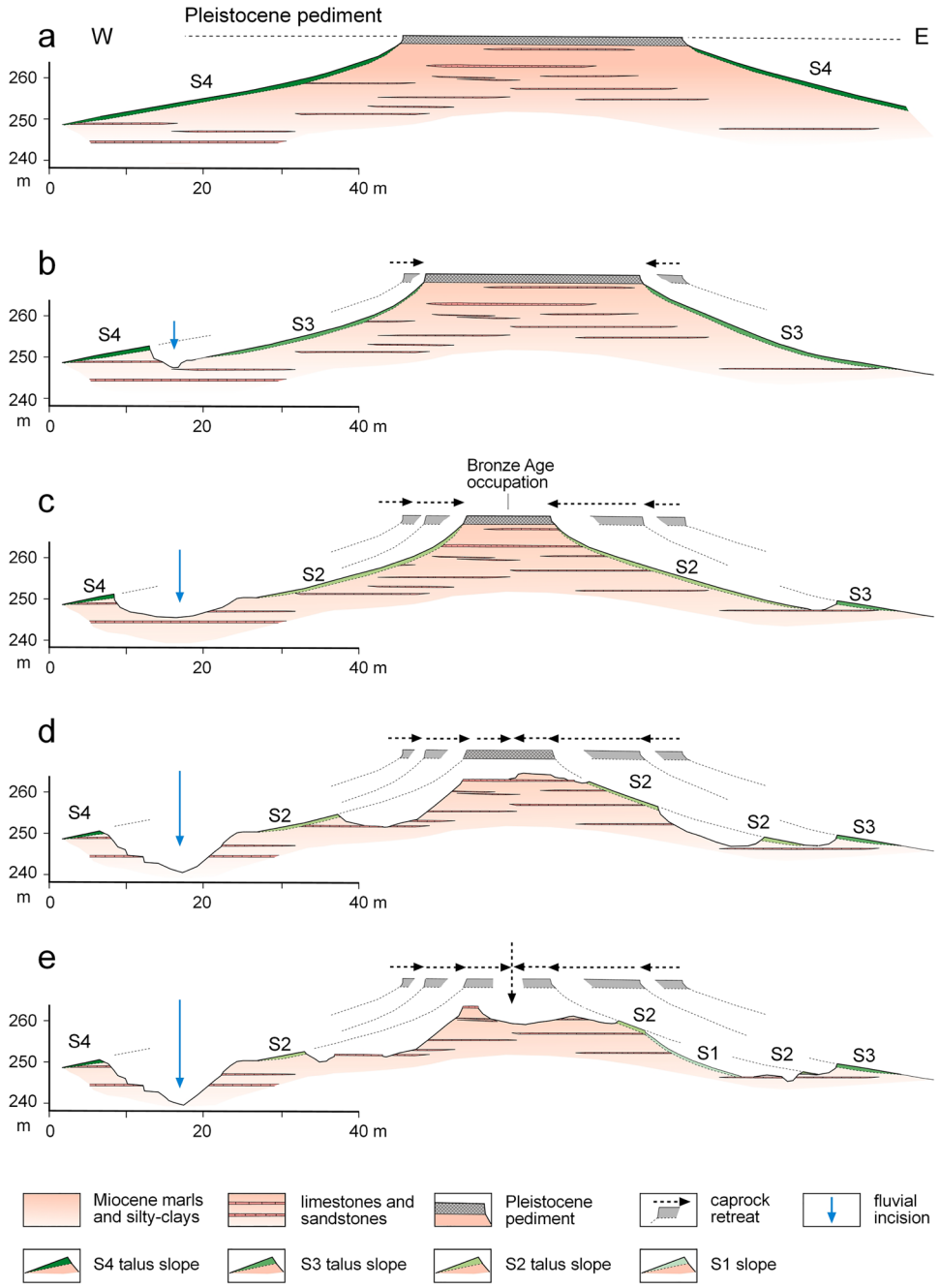

Fig. 12 General evolution of the Jubierre hills: **a** Initial mesa with detritic caprock (Pleistocene pediment) and S4 slope formation; **b** upper caprock retreat and S3 slope stabilisation; **c** S2 slope formation and Bronze Age occupation; **d** erosion of the upper detrital caprock and marls exposure; **e** S1 slope formation, and present evolution of residual hills

from S2 on which it sits. There are few remains of this stage in LPN and Solitario 2.

After the erosion of the upper detrital caprock (Fig. 12d, e), the hard cover was replaced by lower sandstone and limestone layers, as the erosion advanced, as in Solitario 1 (Figs. 3e, 9a), Solitario 2 (Fig. 10a, b), and LPS (Figs. 3d, 7a). As a result, the erosive process slowed. In other cases, the upper protection, such as that on LPN and most of LPS and Solitario 1, was totally lost. This is critical because no other hard Miocene layers are visible and, therefore, erosion occurs quickly.

According to this evolutionary interpretation, the present Jubierre hills (*tozales*) may be in different evolutionary stages. This allows us to classify these hills into three groups (Fig. 13): (a) hills with upper caprock formed by the original gravel deposit; (b) hills with upper caprock formed by inner layers exposed by erosion; and (c) residual hills without caprock (Fig. 13). The first group shows the least evolved hills: the mesas (1 in Fig. 13) and conical hills (2 in Fig. 13). They still have a caprock formed by the cemented calcareous gravels of the Pleistocene pediments; the next stage is represented by the buttes that lost the detrital caprock

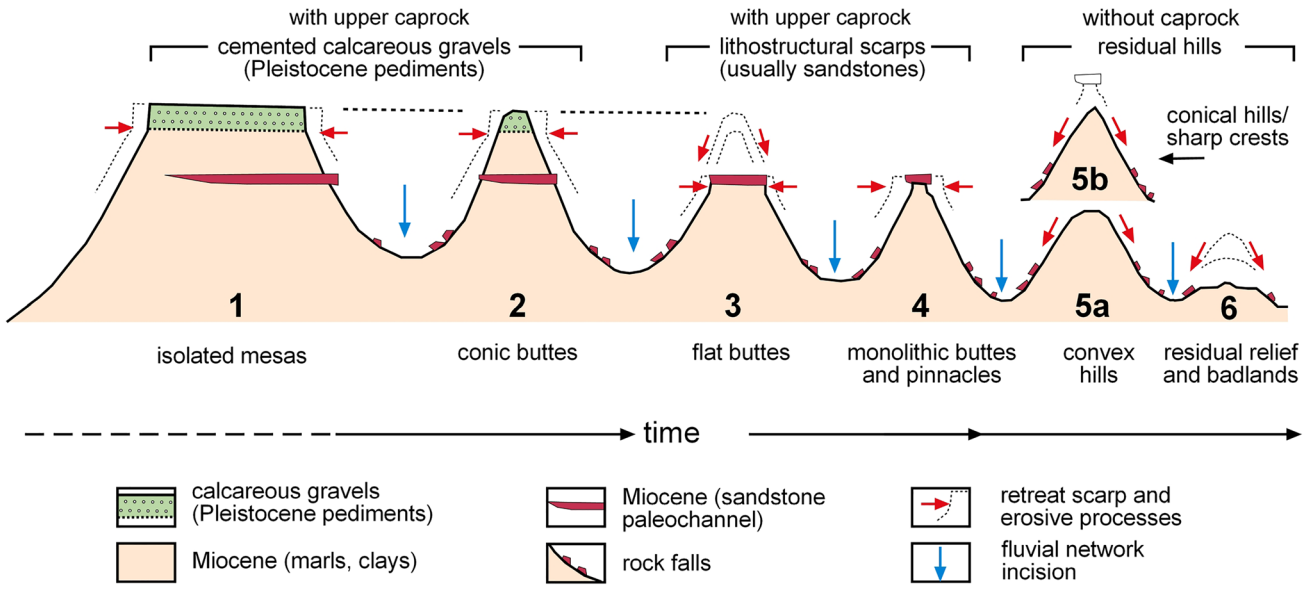

Fig. 13 Interpretation of the type of hills in Jubierre, organised as three main groups according to their evolutionary stage. Explanation in the text

but retain other caprocks formed by resistant lithologies (especially sandstones) lying in positions lower than the cemented gravels (3 in Fig. 13). The scarp retreats gave rise to the development of monolithic buttes and pinnacles (4 in Fig. 13). Finally, after losing the resistant layer, the hill became small mounds modelled on marls and clays shaped as convex hills (5a in Fig. 13) or conical hills and sharp crests (5b in Fig. 13). The rapid erosion of these hills formed badlands and residual reliefs with scattered blocks of old caprocks (6 in Fig. 13).

Talus flatiron stages and interpretation

The relict talus slope or talus flatirons surround the hills as concentric rings, such as those described by Morgan et al. (2008) and Gutiérrez et al. (2015) in Colorado (USA). They are a record of the slopes that enable us to interpret and reconstruct the evolution of the hills. In Jubierre, only S2 slopes have been dated because other stages lack datable materials. Several S2 taluses that are preserved in the four hills analysed include ceramic potsherds from the Bronze Age and these were radiocarbon dated in LPS to 1608–1446 cal BC (Middle Bronze Age). These chronologies coincide with the S2 phase determined by other already cited authors. This type of geoarchaeological relationship with a talus flatiron phase was established in various archaeological sites by Burillo et al. (1981, 1983), Peña Monné and González (1992), Peña Monné and Rodanés (1993), Peña Monné et al. (1996, 2005, 2019), Pérez-Lambán et al. (2014), and Peña Monné 2018). Previous papers shows that this talus flatiron stage developed from the end of the Chalcolithic (4200 BP) to the Iron Age (700–500 BP) and was related to a humid and relatively cold phase that climaxed during the Iron Age Cold Phase or 2.8 event (Bond et al. 1997). Stage S1 was geoarchaeologically defined, but more accurate datings point to the existence of two aggradative phases during the Little Ice Age (Pérez-Lambán et al. 2014; Peña Monné 2018). Although we do not have a dating from Jubierre, this phase is represented by small S2 taluses from LPN, LPS and Solitario 2.

Human occupations occurred on LPN and LPS during the S2 stage around 3500 years ago, when the detrital caprock was still on the hilltop (Fig. 11c). At present, its contemporary talus is between 10 and 25 m from the present hill. This implies a high volumetric loss. These types of estimation are difficult for the older stages, especially with unknown chronologies. However, if the datings of other areas of the Ebro basin are taken into account (Gutiérrez et al. 2010; Peña Monné et al. 2019), the retreat rates for S4 and S3 were relatively slow and this was probably due to caprock protection. From the archaeological point of view, the recent erosive increase accelerates the loss of many archaeological sites located in high places, mainly those from the Bronze Age, Iron Age, and Iberian Epoch. This makes it difficult to reconstruct the peopling of these semiarid environments due to an information loss that is only recoverable using geoarchaeological techniques (Peña Monné 2018).

In general, the evolutionary dynamics of the hills at Jubierre show a predominance of degradative processes, together with the entrenchment of the surrounding ephemeral streams. The development of slopes with thick sediment accumulations reflects interruptions of the generalised

erosive process. Stable periods with cold and wet climatic events point to a climatic cause for these events. The degradative dynamics are recovered with the re-establishment of 'normal' dry and warm conditions, as is the case in the present situation. This is, according to references, the most widely accepted explanation for the formation of S2 and S1 stages, as well as for the intermediate incision phases.

Another variable for the slope Holocene stages is the possible addition of anthropic influence as a new active factor normally triggering or increasing degradative processes. The accumulations remaining from those erosive processes are mainly silts located on the valley floors of Jubierre (Holocene infills in Fig. 2). Results obtained in the Ebro basin show that valley fills started due to slope erosion caused by deforestation in the Neolithic. Sedimentation rates increased with the Bronze Age in some areas and were especially rapid in the Iberian and Roman Epochs (third century BC to fifth century AD) (Constante et al. 2010; Peña Monné et al. 2000, 2004, 2018; Peña Monné 2018). Average sedimentation rates of 4.5 m/kyr were calculated for the Roman Period (Peña-Monné and Sampietro-Vattuone 2019). In conclusion, the incision produced on the S2 slope occurred during the warmer and drier period at the beginning of the Subatlantic and was accelerated by human influence. The combined climatic/anthropic factors are also possible causes of the S1 stage degradation during the Present Warm Period.

Conclusions

The Jubierre reliefs evolved from the conjunction of semi-arid conditions at the centre of the Ebro depression and the dominant soft lithologies. The presence of several stages of talus relict (talus flatirons) generated under wetter than present environmental conditions is an excellent record to reconstruct the geomorphological evolution of the region. Wetter periods from the Upper Pleistocene and Holocene gave rise to stable phases on the slopes with aggradative taluses in the hills. At least four talus flatirons phases can be identified for the development of stabilised slopes (S4 to S1 stages). From these phases, we know the ages of S2 stage (Bond event 2.8, Iron Age Cold Phase) and S1 stage (Little Ice Age) given the presence of archaeological materials. Intermediate incision periods isolated each talus set, and these remain separated from the upper caprock due to erosive retreat. Each talus set remained arranged as concentric rings around the core hill.

The arrangement of the taluses, their composition, gradient, distance from the hills, and inferred morphologies enables a reconstruction of the characteristics, size, height, and position of the original caprock for each stage. Between S4 and S2 stages, the hills maintained similar detrital caprocks (Pleistocene pediments). The scarce remains of the S1 stage show that the caprock was already eroded.

Stage S2 stands out due to human remains that are contemporary to its formation. Ceramic potsherds and the radiocarbon date enable us to establish that this stage developed during (or after) the Middle Bronze Age. Geoarchaeologically, these taluses are the last remaining records for reconstructing past human occupations in these environments.

Acknowledgements This work is a contribution of the "Primeros pobladores y Patrimonio Arqueológico del Valle del Ebro" Aragon Research Group (Government and European Regional Development Fund). This work has partially benefited from financial and technical support provided by the projects CLIP HAR2014-59042-P and HAR2015-65620-P, provided by the Spanish Inter-Ministry Commission of Science and Technology (CICYT); and PICT2018-1119, PICT2019-0931, and PIUNT G629. This paper is within the research scope of IUCA (Environmental Sciences Institute of the University of Zaragoza).

Funding Open Access funding provided thanks to the CRUE-CSIC agreement with Springer Nature. This work was supported by the Spanish Inter-Ministry Commission of Science and Technology (CICYT) (CLIP HAR2014-59042-P and HAR2015-65620-P), the Agencia Nacional de Promoción Científica y Tecnológica (PICT2018-1119 and PICT2019-0931), and the Universidad Nacional de Tucumán (PIUNT G629).

Declarations

Conflict of interest The authors have no relevant financial or non-financial interests to disclose.

References

Bond G, Showers W, Cheseby M, Lotti R, Almasi P, deMenocal P, Priore P, Cullen H, Hajdas I, Bonani G (1997) A pervasive millennial-scale cycle in North Atlantic Holocene and glacial climates. Science 278:1257–1266

Boroda R, Amit R, Matmon A, Finkel R, Porat N, Enzel Y, Eyal Y (2011) Quaternary-scale evolution of sequences of talus flatirons in the hyperarid Negev. Geomorphology 127:41–52. https://doi.org/10.1016/j.geomorph.2010.12.003

Boroda R, Matmon A, Amit R, Haviv I, Arnold M, Aumaître G, Bourlès DL, Keddadouche K, Eyal Enzel Y, Yehouda E (2014) Evolution and degradation of flat-top mesas in the hyper-arid Negev,

Israel revealed from 10Be cosmogenic nuclides. Earth Surf Process Landf 39:1611–1621
Burillo F, Peña Monné JL (1984) Clima, geomorfología y ocupación humana. Introducción a un planteamiento metodológico. In: Actas Iª Jornadas de Metodología de Investigación Prehistórica, Soria, pp. 91–102
Burillo F, Gutierrez M, Peña Monné JL (1981) El Cerro del castillo de Alfambra (Teruel). Estudio interdisciplinar de Geomorfología y Arqueología. Kalathos 1:7–63
Burillo F, Gutiérrez M, Peña Monné JL (1983) La Geoarqueología como ciencia auxiliar. Una aplicación a la Cordillera Ibérica Turolense. Revista De Arqueología 26:6–13
Calle M, Sancho C, Peña JL, Cunha P, Oliva-Urcía B, Pueyo E (2013) La secuencia de terrazas cuaternarias del río Alcanadre (provincia de Huesca): caracterización y consideraciones paleoambientales. Cuad. Invest. Geográfica 39(1):159–178. http://dx.doi.org/https://doi.org/10.18172/cig.2004
Constante A, Peña-Monné JL, Muñoz A (2010) Alluvial geoarchaeology of an ephemeral stream: implications for Holocene landscape change in the Central part of the Ebro depression. Northeast Spain Geoarchaeology 25(4):475–496. https://doi.org/10.1002/gea.2031
Cuadrat JM, Saz Sánchez MA, Vicente SM (2007) Atlas climático de Aragón. Gobierno de Aragón, Zaragoza
Duszyński F, Migoń P, Strzelecki MC (2019) Escarpment retreat in sedimentary table-lands and cuesta landscapes – landforms, mechanisms and patterns. Earth Sci Rev 196:102890. https://doi.org/10.1016/j.earscirev.2019.102890
Gerson R, Grossman S (1987) Geomorphic activity on escarpments and associated fluvial systems. In: Rampino MR, Sanders JE, Newman WS, Königsson LK (eds) Climate, History, Periodicity and Predictability. Reinhold, New York, pp 300–322
Gutiérrez M, Peña Monné JL (1993) Depresión del Ebro. In: Guriérrez M (ed) Geomorfología de España. Rueda, Madrid, pp 305–349
Gutiérrez M, Peña Monné JL (1998) Geomorphology and late Holocene climatic change in northeastern Spain. Geomorphology 23:205–217
Gutiérrez M, Lucha P, Gutiérrez F, Moreno A, Guerrero J, Martín-Serrano A, Nozal F, Desir G, Marín C, Bonachea J (2010) Are talus flatiron sequences in Spain climate-controlled landforms? Z Geomorphol 54:243–252. https://doi.org/10.1127/0372-8854/2010/0054-0013
Gutiérrez F, Morgan ML, Matthews V, Gutiérrez M, Jiménez-Moreno G (2015) Relict slope rings and talus flatirons in the Colorado Piedmont: origin, chronology and paleoenvironmental implications. Geomorphology 231:146–161. https://doi.org/10.1016/j.geomorph.2014.11.024
Hackney CH, Clayton A (2015) Unnamed aerial vehicles (UAVs) and their application in geomorphic mapping. In: Cook S, Clarke L, Nield J (eds) Geomorphological techniques, chap. 2, sec. 1.7. British Soc. for Geomorphology, London, pp 1–12
Hirst JPP, Nichols GJ (1986) Thrust tectonic controls on Miocene alluvial distribution patterns, southern Pyrenees. In: Allen P, Homewood P (eds) Foreland basins. International Association of Sedimentologist Special Publications, Washington, pp 247–258
Jorayev G, Wehr K, Benito-Calvo A, Njau J, de la Torre I (2016) Imaging and photogrammetry models of Olduvai Gorge (Tanzania) by unmanned aerial vehicles: a high-resolution digital database for research and conservation of Early Stone Age sites. J Archaeol Sci 75:40–56
Meléndez A, Alonzo-Zarza AM, Sancho C (2011) Multi-storey calcrete profiles developed during the initial stages of the configuration of the Ebro Basin's exorrheic fluvial network. Geomorphology 134:232–248
Migoń P, Różycka M, Jancewicz K, Duszyński F (2018) Evolution of sandstone mesas following landform decay until death. Prog Phys Geogr 42:588–606
Migoń P, Duszyński F, Jancewicz K, Różycka M (2019) From plateau to plain – using ergodic assumption in interpreting geoheritage through a thematic trail, Elbsandsteingebirge, Germany. Geoheritage 11:839–855
Migoń P, Duszyński F, Jancewicz K, Kotwicka W (2020) Late evolutionary stages of residual hills in tablelands (Elbsandsteingebirge, Germany). Geomorphology 367:107308. https://doi.org/10.1016/j.geomorph.2020.107308
Morgan ML, Matthews V, Gutiérrez F, Thorson JP, Madole RF, Hanson PR (2008) From buttes to bowls: repeated relief inversión in the landscape of the Colorado Piedmont. In: Raynolds RG (ed) Roaming the rocky mountains and environs. Geological field trips. Geological Society of America Field Guides, pp 203–215
Oh JS, Seong YB, Larson PH, Hong SC, Yu BY (2019) Asymmetric hillslope retreat revealed from Talus flatirons on rock peak, San Tan mountains, Arizona, United States: assessing caprock lithology control on landscape evolution. Ann Am Assoc Geogr 110(1):98–119. https://doi.org/10.1080/24694452.2019.1624421
Orton C, Tyers P, Vince A (1993) Pottery in archaeology. Cambridge University Press, Cambridge
Pardo G, Arenas C, González A, Luzón A, Muñoz A, Pérez A, Pérez-Rivarés FJ, Vázquez-Urbez M, Villena J (2004) La cuenca del Ebro. In: Vera JA (ed) Geología de España. IGME and Sociedad Geológica de España, Madrid, pp. 533-543
Peña Monné JL (1997) Cartografía geomorfológica básica y aplicada. Ed. Geoforma, Logroño, 235 pp
Peña Monné JL (2018) Geoarqueología aplicada a la reconstrucción paleoambiental: La evolución del Holoceno superior en el NE de España. Boletín Geológico y Minero 129(1/2): 285–303. http://doi.org/https://doi.org/10.21701/bolgeomin.129.1.011
Peña Monné JL, González JR (1992) Hipótesis evolutiva de los cambios en la dinámica geomorfológica del Baix Cinca y Segre (Depresión del Ebro) durante el Pleistoceno superior-Holoceno a partir de los datos geoarqueológicos. Cuaternario y Geomorfología 6: 103-110
Peña Monné JL, Rodanés JM (1993) Evolución geomorfológica y ocupación humana en el cerro de Masada de Ratón (Baix Cinca, prov. de Huesca). Cuaternario y Geomorfología 6: 81-89
Peña-Monné JL, Sampietro-Vattuone MM (2019) Late Holocene anthropic degradation records in semi-arid environments (NE Spain and NW Argentina). Geogr Res Lett 45(1):195–217. https://doi.org/10.18172/cig.3587
Peña Monné JL, González Pérez JR, Rodríguez Duque JI (1996) Paleoambientes y evolución geomorfológica en yacimientos arqueológicos del sector oriental de la Depresión del Ebro durante el Holoceno superior. In: Pérez Alberti A, Martini P, Chesworth W, Martínez Cortizas A (coord) Dinámica y Evolución de medios Cuaternarios. Xunta de Galicia, Santiago de Compostela, pp. 63–80
Peña-Monné JL, Echeverría MT, Chueca J, Julián A (2000) Processus d´accumulation et d´incision pendant l´Antiquité Classique dans la vallée de la Huerva (Bassin de l´Ebre, Espagne). In: Vermeulen F (ed) Geoarchaeology of the Landscapes of Classical Antiquity. Editorial Peters, Leuven, pp. 151-159
Peña Monné JL, Julián A, Chueca J, Echeverría MT, Ángeles G (2004) Etapas de evolución holocena en el valle del río Huerva: Geomorfología y Geoarqueología. In: Peña-Monné JL (eds) Geografía Física de Aragón. Aspectos generales y temáticos. Univ. Zaragoza e Inst. Fernando el Católico, Zaragoza, pp. 289-302
Peña Monné JL, Sampietro Vattuone MM, Longares Aladrén LA, Pérez Lambán JV, Sánchez Fabre M, Alcolea Gracia M, Vallés L,

Echeverría MT, Baraza C (2018) Holocene alluvial sequence of Valderazagoza (Los Monegros) in the paleoenvironmental context of the Ebro Basin (Spain). Geogr Res Lett 44(1):321–348. https://doi.org/10.18172/cig.3358

Peña-Monné JL, Rubio-Fernández V, Sampietro-Vattuone MM, García Giménez R (2019) Relict slopes and palaeovalleys at Taracena-Guadalajara (Central Spain): Geomorphological and palaeogeographical interpretation. Palaeogeography, Palaeoclimatology, Palaeoecology 540: 106855. https://doi.org/10.1016/j.yebeh.2019.106855

Pérez-Rivarés FJ, Garcés M, Arenas C, Pardo G (2003) Magnetocronología de la sucesión miocena de la Sierra de Alcubierre (sector central de la cuenca del Ebro). Rev Soc Geol España 15(3-4): 217-231

Pérez-Lambán F, Peña-Monné JL, Fanlo J, Picazo JV, Badia D, Rubio V, García-Jiménez R, Sampietro-Vattuone MM (2014) Paleoenvironmental and geoarchaeological reconstruction from late Holocene slope records (Lower Huerva Valley, Ebro Basin, NE Spain). Quat Res 81:1–14. https://doi.org/10.1016/j.yqres.2013.10.011

Picazo Millán JV (1993) La Edad del Bronce en el Sur del Sistema Ibérico Turolense, I: Los Materiales Cerámicos. Monografías Arqueológicas del SAET, 7, Teruel

Quirantes J (1978) Estudio sedimentológico del Terciario continental de los Monegros. Institución Fernando el Católico, Zaragoza

Ramírez JI, Solá Subiranas J (1990) Mapa Geológico de España serie MAGNA escala 1:50000, hoja 386, Peñalba. I.G.M.E., Madrid

Rodríguez-Ochoa R, Olarieta JR, Santana A, Castañeda C, Calle M, Rhodes E, Bartolomé M, Peña-Monné JL, Sancho C (2019) Relict periglacial soils on quaternary terraces in the Central Ebro Basin (NE Spain). Permafr Periglac Process 30(4):364–373. https://doi.org/10.1002/ppp.2005

Sancho C, Gutiérrez M, Peña JL, Burillo F (1988) A quantitative approach to cliff retreat starting from triangular slope facets, central Ebro Basin, Spain. Catena Suppl 13:139–146

Sancho C, Meléndez A (1992) Génesis y significado ambiental de los caliches pleistocenos de la región del Cinca (Depresión del Ebro). Rev Soc Geol España 5: 81-93

Schmidt KH (1994) Hillslopes as evidence of climatic change. In: Abrahams AD, Parsons AJ (eds) Geomorphology of desert environments. Chapman and Hall, London, pp 553–570

Sheeland CE, Ward DJ (2018) Late Pleistocene talus flatiron below the Coal Clift cuesta, Utah, USA. Earth Surf Proc Land 43(9):1973–1992. https://doi.org/10.1002/esp.4369